Lu Cheng, Yi Xi*, Chenguo Hu, Xule Yue and Guo Wang

Ag Nanowires Single Electrode Triboelectric Nanogenerator and Its Angle Sensors

DOI 10.1515/ehs-2015-0012

Abstract: As we known, nanogenerator (NG) can be used in many fields, such as sensors, energy harvesting, biomedical application, and so on. Sometimes, the object that is a part of NG cannot be electrically connected to the load because it is a mobile object. To harvest energy from such a case and reduce the fabrication cost and achieve some new applications such as touch screen products, we need to find new method to fabricate NG. To attain the higher output current and output power, moreover, here we report a flexible and easy fabricated single electrode triboelectric nanogenerator (TENG) based on polydimethylsiloxane (PDMS) and silver (Ag) nanowires (NWs). Due to Ag NWs high specific surface area, the electrical conductivity of Ag NWs is better than the block of Ag, and PDMS is the transparent and flexible. The single electrode TENG not only can harvest energy from environment but also is a self-powered sensor for detecting acceleration from different angles. This TENG can attain an open-circuit voltage up to 330 V, a maximum short-circuit current of 15.5 μ A (2.6 μ A/cm^2) and a maximum power of 1.5 mW (0.25 mW/cm^2) on the load of 20 MΩ.

Keywords: single electrode, TENG, Ag NWs, polydimethylsiloxane (PDMS)

Introduction

Over the past decades, for meeting the demands of rapid-growing energy consumptions, scientists make great efforts to find renewable and green energy. And in our daily life, there are many kinds of ubiquitous and accessible mechanical energies in human's movements, such as human being's walking, driving and the machine's operating, etc. Therefore, how to harvest these mechanical energies efficiently has attracted researchers' attentions for its potential applications. Nanogenerator (NG) (Wang and Song 2006; Yang et al. 2009; Gu et al. 2013; Jung et al. 2012; Guo et al. 2014) a unique technology for harvesting energy based on electromagnetic (Rome et al. 2005; Williams et al. 2001), electrostatic (Herb, Parkinson, and Kerst 1937; Mitcheson et al. 2004) and piezoelectric (Lee et al. 2013; Shin et al. 2014) mechanisms has been found to meet this demand. Thus, researchers around the world dedicated themselves to develop self-powered electronic devices based on electromagnetic, electrostatic and piezoelectric effects (Park et al. 2010; Gao et al. 2007; Ko et al. 2014). NG, especially triboelectric nanogenerator (TENG) (Fan, Tian, and Wang 2012; Lin et al. 2013; Jing et al. 2014), has been regarded as one of promising invents for its capable of harvesting energy from the environment in order to converting mechanical energy into electrical energy.

However, most of TENGs are the separation of two electrodes based on coated on the triboelectric thin film materials for output. Sometimes, the object that is part of the TENG cannot be electrically connected to the load because it is a mobile object, such as a human walking on a floor (Wang 2014). To harvest energy from such a case and reduce the fabrication cost and achieve some new applications such as touch screen products, we need to find new method to fabricate TENG. The most effective method is we can fabricate a kind of electrode TENG without the need of coating the metal electrodes on triboelectric film materials. This type of TENG can be applied for touch screen and harvest energy from touching, pushing and striking, etc.

According to the coupling between the triboelectric effect and the electrostatic effect, the periodic contact-separation between object and surface of polydimethylsiloxane (PDMS) thin layer results in charges transfer between Ag NWs electrode and the ground. In addition, the friction effect between Ag NWs and PMDS may enhance the output of the TENG. In this paper, we fabricated a new and simple single electrode TENG (Zhang et al. 2014a, 2014b; Yang et al. 2013a, 2013b, 2013c) based on PDMS by using Ag nanowires (NWs) as electrode. This fabricated TENG can produce an open-circuit voltage up to 330 V and a maximum short-circuit current of 15.5 μA, which lead to the maximum power of 1.5 mW at a load of 20 ΩM. Moreover, the TENG can light almost 30 green light-diodes (LEDs) during the periodic motion. And this

***Corresponding author: Yi Xi,** Department of Applied Physics, Chongqing University, Chongqing 400044, China, E-mail: yxi6@cqu.edu.cn
Lu Cheng, Chenguo Hu, Xule Yue, Guo Wang, Department of Applied Physics, Chongqing University, Chongqing 400044, China

TENG has been used as self-powered sensor for detecting the movement of an object from different angles. And through the signal we obtain, we can know the movement from different angles.

Experimental Section

The Method of Synthesis Ag NWs

To obtain high-quality Ag NWs (Ding et al. 2012; Sun and Xia 2002), $AgNO_3$ and PVP were used as starting materials. $AgNO_3$ (Aldrich, 99%) was dissolved in distilled water to form a 0.25 M $AgNO_3$ aqueous solution. And PVP (weight-average molecular weight 55,000, Aldrich) was dissolved in deionized water to obtain a 0.375 M PVP aqueous solution. Ag NWs were synthesized as fellows: First, 30 ml of anhydrous ethylene glycol (Aldrich, 99.8%) was heated at 160°C for 1 h in oil bath pat. Second, 18 ml of $AgNO_3$ aqueous solution and 18 ml of PVP aqueous solution were simultaneously introduced in anhydrous ethylene glycol by means of acid-type burette at a rate of 1 ml/min. The mixture solution was continued to heating at 160°C for another 45 min under magnetically stirring. Finally, the mixture solution was washed by ethanol for several times until obtaining the cleaned Ag NWs.

Synthesis of $NaNbO_3$ NWs

$NaNbO_3$ NWs can be synthesized by hydrothermal method (Jung et al. 2011). 8 g of NaOH was dissolved into 20 ml of deionized water under magnetically stirring to form a 10 M NaOH aqueous solution. Then 1 g of Nb_2O_5 was added into the NaOH solution. After stirring for 30 min, the mix solution was removed into a 25 ml Teflon lining in a stainless steel autoclave. The autoclaves were placed into oven at 150°C for 16 h. Until the oven was natural cooling to the room temperature, we can get the white floccules. And after the white floccules (Ke et al. 2008) was filtered, washed with distilled water several times until PH $=$ 7, we obtained as-prepared powders dried at 80°C for 12 h. And then we got the final products after annealing at 600°C for 12 h.

Fabrication of the Single Electrode TENG

The fabrication started by PDMS polymer. To form the PDMS thin layer, 1 g fluidic PDMS polymer mixture was prepared by mixing base and curing agents in the ratio of 10:1, and the mixture PDMS polymer was poured into the mold which was placed on the glass plate. The size of the mold is 4 cm $\times$ 4 cm $\times$ 0.2 cm, and then cured at 55°C for 30 min in an oven. The semi-cured PDMS thin layer was deposited on Ag NWs as an electrode. Finally, the other 1 g fluidic PDMS polymer mixture covered on the top of the Ag electrode. And after fully curing the PDMS for one day, we obtain the single electrode TENG. Specially, Cu wire is connected with Ag electrode by using Ag paste, and the total thickness of the TENG is about 500 μm.

Characterization and Measurement of the Single Electrode TENG

The morphology, chemical composition, and the structure of products were characterized by field-emission scanning microscopy (Nova 400 Nano SEM), X-ray diffraction (XRD) measurement with Cu Kα radiation (wavelength 1.5418 Å) at a 2°$\min^{-1}$ speed was used to study the crystal phase. And the TENG was driven by linear monitor, the output performance of the TENG is measured by a Stanford low-noise current preamplifier (Model I SR570) and a data acquisition card (NI PCI-6259).

Results and Discussion

Figure 1(a) shows SEM image of Ag NWs, the length of Ag NWs is about 20 μm. And the insert in Figure 1(a) shows EDS image of the Ag NWs. And XRD pattern of Ag NWs was shown in Figure 1(b), which present the sample is Ag crystalline. And the SEM image and XRD pattern of $NaNbO_3$ NWs show in Figure 1(c) and (d), respectively, the length of $NaNbO_3$ NWs is also 10~20 μm. The detailed process of fabricating the TENG based on PDMS is schematically shown in Figure 2(a)–(c). The mixture fluidic PDMS polymer was poured into the mold which was fixed on the glass plate to form the PDMS thin layer, as shown in Figure 2(a). Ag NWs was deposited on semi-cured PDMS thin layer that served as electrode (Figure 2(b)), which replaced another traditional electrode just like Al, Cu and so on. To avoid Ag NWs dropping out from PDMS polymer thin film on excessive mechanical straining, the other mixture fluidic PDMS polymer covered on the top of the Ag electrode to fabricate the PDMS-Ag-PDMS structure (Figure 2(c)). Figure 2(d) and (e) shows the top view SEM image and cross-sectional after Ag NWs depositing

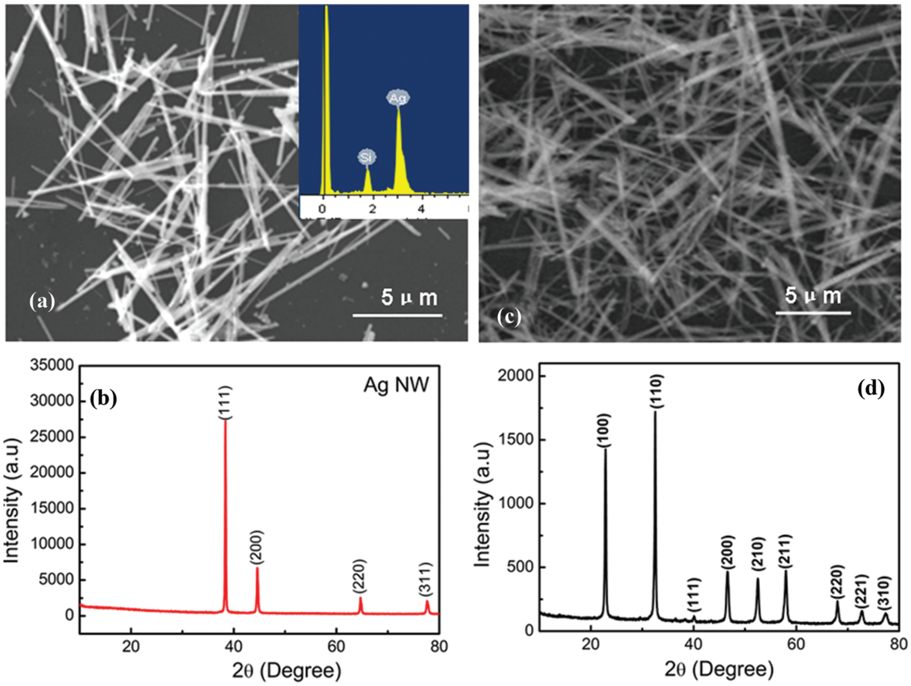

Figure 1: (a) SEM image of Ag NWs, the inset is the EDS image of Ag NWs (b) XRD pattern of Ag NWs. (c) and (d) the SEM image and XRD pattern of $NaNbO_3$ NWs, respectively.

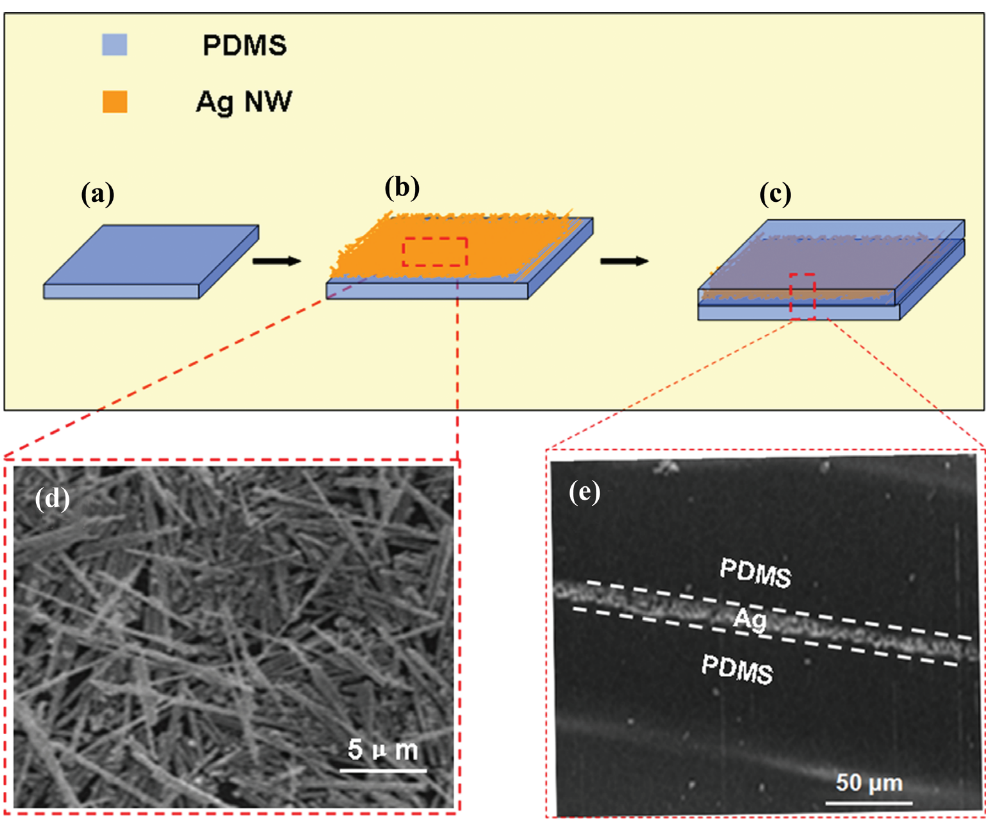

Figure 2: (a)–(c) Schematic diagrams of the NG fabrication process (a) PDMS thin layer substrate (b) Ag NWs depositing on PDMS layer as electrode (c) PDMS polymer mixture covered on the top of electrode (d) SEM image of Ag NWs distributed on PDMS thin layer. (e) SEM image of cross-section of the PDMS-Ag-PDMS structure.

on the PDMS thin layer, respectively. And the top view image shows Ag NWs were randomly oriented and well-distributed without aggregations.

Figure 3(a)–(d) illustrates the working mechanism of the single-electrode TENG based on PDMS by the contact electrification and electrostatic induction. In the original state, the object and PDMS completely contact each other; consequently, the free charges transfer both of them. According to the triboelectric series, electrons were injected from the object to PDMS surface due to PDMS is more triboelectrically negative than the object. There is no electrons flow in the external load according to the electrostatic equilibration between PDMS and object, just as presented in Figure 2(a). When the object gradually separate from the surface of PDMS, these triboelectric charges cannot be balanced any more. The negative charges on the surface of the PDMS can induce the positive charges on the Ag NWs electrode, leading to a flow of free electrons from Ag NWs electrode to the ground, as shown in Figure 3(b). This electrostatic inducting process can generate an output short-circuit current. With the separation distance of the object and the PDMS increasing, the negative charges on the PDMS and the positive charges on the Ag NWs electrode achieve a new electrostatic equilibration; consequently, there is no output signal can be observed, as depicted in Figure 3(c). And when the object approach the PDMS again, the positive charges on Ag NWs electrode decrease and the free electrons flow from the ground to the electrode until the object and PDMS completely contact again, leading to the opposite short-circuit current signal, as illustrated in Figure 3(d).

To study the influencing factors of the TENG, we make contrasts of the thinness, the quantity of Ag NWs as well as electrode materials for three groups, as shown in Figure 4. To further investigate the effect of the thickness of the PDMS, it varied from 1.0 mm to 2.0 mm under the pushing frequency of 2.5 Hz. At each thickness, the output currents were obtained as about 10.3 μA, 9.6 μA and 6.5 μA, respectively, as shown in Figure 4(a). It is proved that the output short-circuit current gradually decreases with the increasing thickness of the PDMS. This indicates the thickness of PDMS can influent the output of the single electrode TENG. Figure 4(b) displays the different amount of Ag NWs with the same thinness of PDMS. From this result, we can see that the output currents are increased with increasing the amount of Ag NWs. By 2.5 Hz of pushing frequency, the currents were

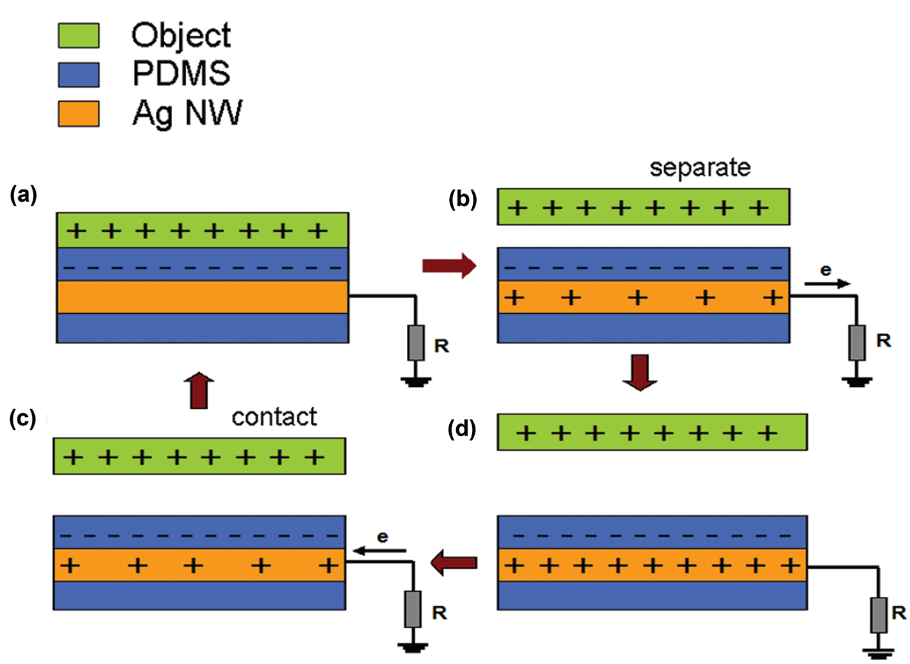

Figure 3: The working principle of the single-electrode TENG. (a) In original state, positive and negative triboelectric charges are produced on the Ag NWs electrode and PDMS polymer side, respectively (b) The gradual separation between the surface of PDMS and the object. The unbalance between Ag electrode and PDMS drives electrons flowing from Ag electrode to the ground. (c) The electrostatic equilibration between PDMS and Ag electrode. (d) Electrons are driven back from the ground to the Ag electrode due to the decreased separation.

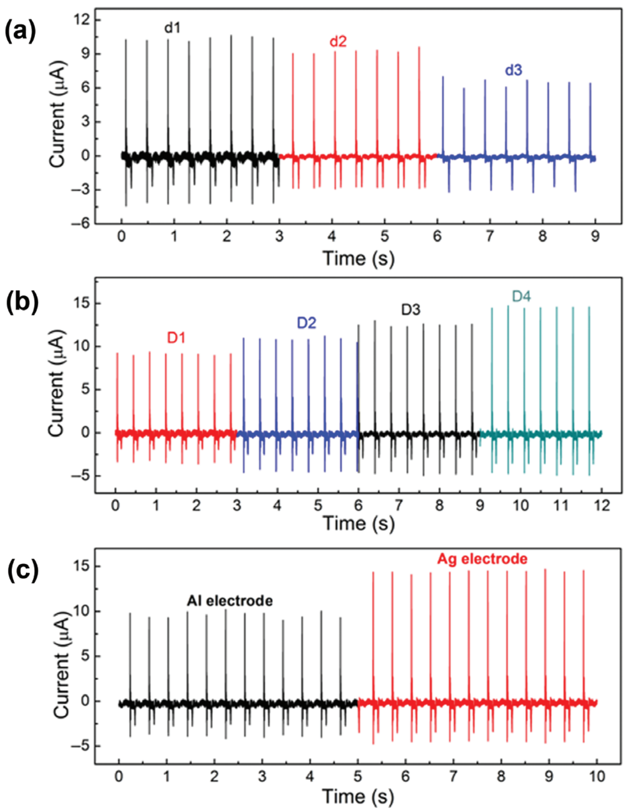

Figure 4: (a) The short-circuit currents produced by the PDMS-based triboelectric nanogenerator with the different thinness of PDMS layer and the same amount of Ag NWs under external pushing frequency of 2.5 Hz. The thickness of PDMS layer d1, d2, d3 is 1 mm, 1.5 mm, 2 mm, respectively. (b) The different amount of Ag NWs with the same thinness of PDMS. (c) The contrast between Ag NWs electrode and the traditional conductive material-aluminum.

increased from 9.1 μA to 15.5 μA. This can be explained by the fact more Ag NWs can increase the amount of the generated triboelectric charges because of the high specific area of Ag NW. To examine the difference from the Ag NWs electrode and traditional electrode, we choose Al as contrast electrode in Figure 4(c). From this result, we can observe clearly that the performance of traditional electrode is not good enough than Ag NWs electrode. And the output currents are almost 10 μA and 15.5 μA, respectively. These results are prior to another research of TENG based on PDMS.

Figure 5 shows the performance of this TENG. The highest output current of TENG is about 15.5 μA and was demonstrated in Figure 5(a). This TENG can light up 30 commercial LEDs without using the energy storage, as shown in the digital image in the inset of Figure 5(a). And the output voltage on the external load resistance of 300 MΩ was shown in Figure 5(b). To further investigate the relationship of the output current and voltage of single electrode TENG based on PDMS, we used different resistors as external loads in Figure 5(c), the current drops with increasing load resistance, meanwhile, the voltage rises. As displayed in Figure 5(d), the instantaneous peak power of 1.5 mW is maximized at a load resistance of 20 MΩ.

Figure 6 shows the influence of different amount of $NaNbO_3$ NWs and Ag NWs on the output of TENG. Figure 6(a) shows the output current of the single electrode TENG using pure $NaNbO_3$ NWs without Ag NW under the pushing frequency of 2.5 Hz. It implied that the more $NaNbO_3$ NWs the higher the output current was measured. Figure 6(b) represents the output current of the layer-by-layer structure of Ag NWs/$NaNbO_3$ on PDMS. And in Figure 6(b), it indicated that the addition of same amount of Ag NWs can increased the output of TENG, and the amount of the $NaNbO_3$ NWs also was important influencing factor for the measured output. And compared to Figure 6(a), the output with Ag NWs was 4~80 times than without Ag NWs, as shown in Figure 6(b). The reason accounting for this consequence mostly is $NaNbO_3$ NWs could be decreasing the inducing charges from the surface of PDMS.

To further explore the influence of the amount Ag NWs, the different amounts of Ag NWs as electrode were measured in Figure 6(c) and 6(d). Figure 6(c) shows the measured output current of the different amount Ag NWs with the same $NaNbO_3$ NWs layer by layer. And the output of TENG generated by using the pure Ag NWs as electrode was shown in Figure 6(d).These results can be explained that the output of the single electrode TENG was influent by conductive materials.

To illustrate the potential application of the Ag NWs single-electrode TENG to harvest mechanical energy in daily life, we demonstrated the TENG can be used as a self-powered sensor for detecting the movement from different angles. We fabricated a TENG with the size of 3 cm × 3 cm, and the TENG was placed on a plastic plate, which was fixed on the bottom of a transparent plastic tube. And this tube was fixed with hob machine. A PTFE ball move along the wall of the tube until reached the bottom freely. When the ball contacted to the TENG, the output current of the TENG can be observed. We measured the output current of the TENG under different tilt angles (defined as the angles between the ground and the plastic tube), as shown in Figure 7(a). Figure 7(c)–(f) shows the output currents under different angles of 30°,

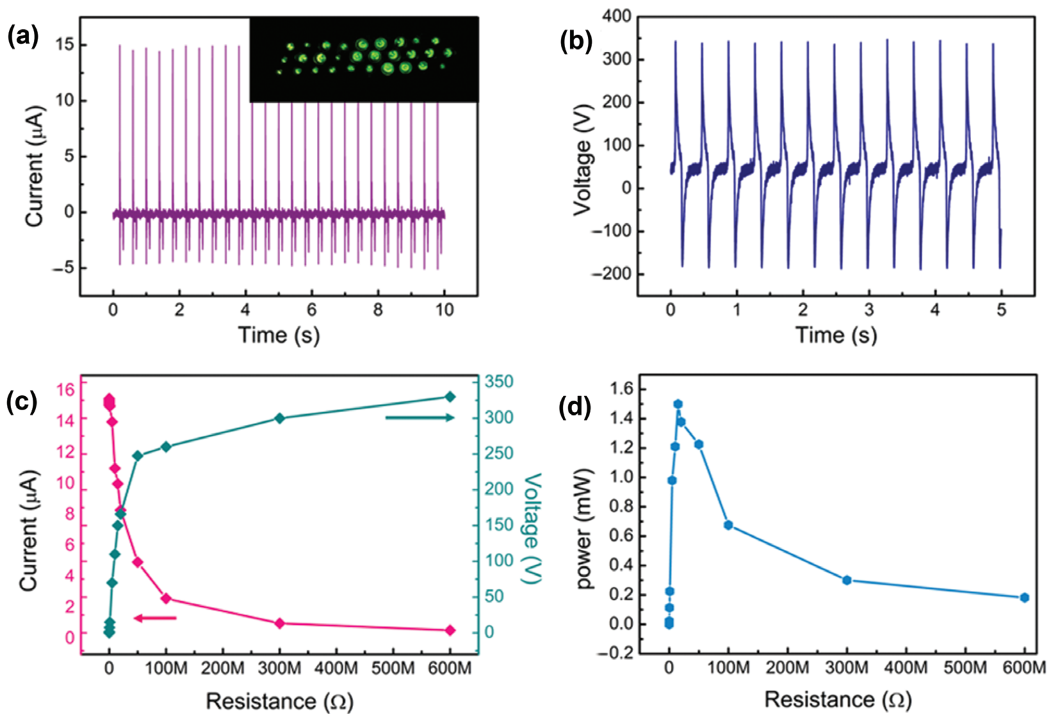

Figure 5: The electrical performance of the TENG under pushing frequency of 2.5 Hz and an impelling amplitude of 2.4 cm. (a) The current-curve for single electrode TENG as a power to light up 30 commercial LEDs. The inset is the photograph of LEDs driven by the TENG. (b) The voltage output on the external load resistance of 300 MΩ. (c) Dependence of the voltage and current output on the external load resistance for the TENG (d) the peak power output on the resistance of the external load for the TENG, implying maximum power output of 1.5 mW on the load of 20 MΩ.

45°, 60°, 90°, respectively, there are several peaks in each figure. The first peak we observed was the first time the PTFE ball contacting to the TENG, and the rest of peaks are due to the elastic of the PTFE ball. In the process of the speed of the ball reducing to zero, the ball will contacted the TENG because of the elastic collision until the speed of the ball reducing to zero. Furthermore, the contacting time was relative to the tilt angle of the tube and we can calculate the average force ($\bar{F}$) the ball generating according to the total contacting time. And the maximum current can be up to ~1.2 μA at the tilt angle of 90°.

$$\mathrm{V} = \sqrt{2gh\cos\theta} \quad [1]$$

$$\bar{F} = \mathrm{mV}/\Delta\mathrm{t} \quad [2]$$

g represents acceleration of gravity, h represents the length of the transparent tube, θ represents the tilt angle of the tube, $\bar{F}$ represents the average force the ball generating, m represents the weight the ball, V represents the speed of the ball contacting the TENG first time and Δt represents the total contacting time. According to the formulas (1) and (2), we get the relationship as follows (Table 1).

Figure 7(g) shows the plot of the output currents versus the tilt angle of the tube. Because of the increase of the gravity acceleration of the PTFE ball, it moves faster and faster with increasing tilt angles, leading to the increasing output current of the TENG.

Conclusion

In summary, we have demonstrated a flexible, easy fabricated and low-cost single electrode TENG consisting of PDMS and Ag NWs. Ag NWs were utilized as electrode replacing traditional electrodes such as Al, Cu, etc. In addition, the periodic contact/separation between the object and PDMS film results in the output of the TENG. And the TENG produces an open-circuit voltage up to 330 V, a short-circuit current of 15.5 μA, and a maximum power of 1.5 mW on load resistance of 20 MΩ, which can lighted up about 30 LEDs. Moreover, the single

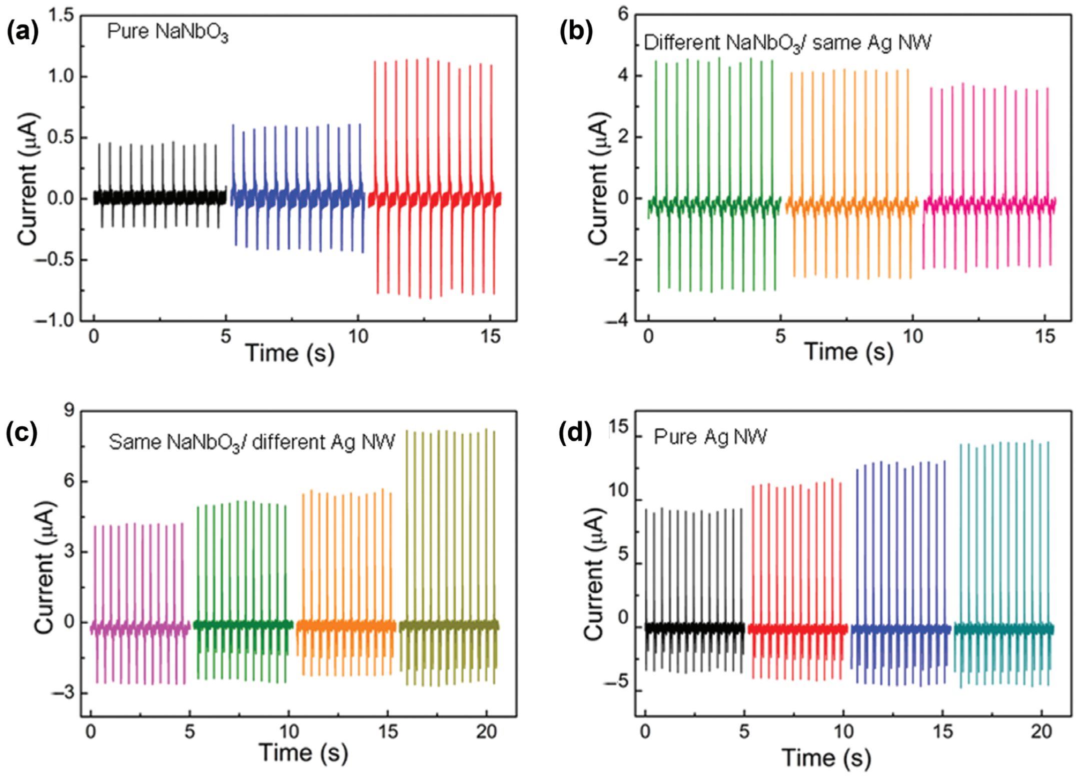

Figure 6: (a) Measured short-circuit currents of single-electrode TENG using different amounts of pure $NaNbO_3$ NWs as electrode, with the volume weight ratio of 1:2:3. (b) On the basis of (a), measured short-circuit currents of single electrode TENG with the same amount of Ag NWs. (c) Measured short-circuit currents of single electrode TENG using different amounts of Ag NWs as electrode. (d) On the basis of (c), measured short-circuit currents of single electrode TENG with the same amount of $NaNbO_3$ NGs.

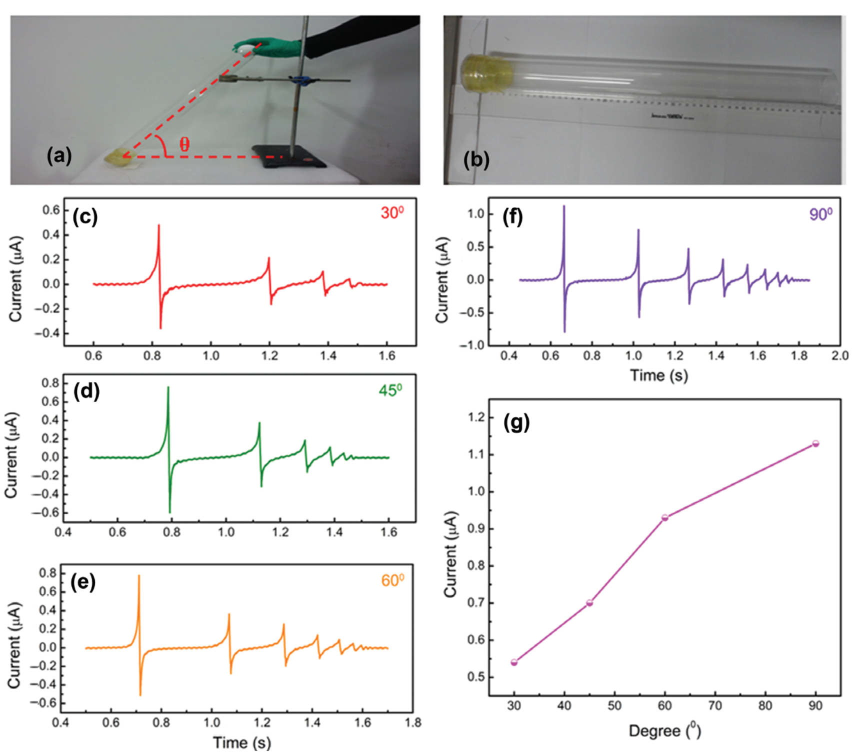

Figure 7: (a) The optical image of the application of the single electrode TENG. (b) The photograph of the length of the plastic tube. (c)–(e) the short-circuit currents measured under the different angles. And the value of angles is 30°, 45°, 60°, 90°, respectively. (g) The plot of the output current versus the tilt angle of the tube.

Table 1: The relationships between the angle, the average force and the output current.

Angle	30°	45°	60°	90°
Total contacting time (Δt)	0.7 s	0.8 s	0.9 s	1.0 s
The average force ($\bar{F}$).	0.211 N	0.230 N	0.226 N	0.219 N
Output current	0.54 μ A	0.77 μ A	0.95 μ A	1.20 μ A

electrode TENG can be used as sensor to detecting the different angle via observing the signal of the TENG generating. After calculation, we can conclude that with the increasing of the angle, the output of the TENG is increasing. And the TENG can produces short-circuit current of almost 1.2 μA at the angle of 90°.

Funding: This work has been funded by the NSFC (11204388), the SRFDP (20120191120039, 20110191110034), the large-scale equipment sharing fund of Chongqing University, and the Fundamental Research Funds for the Central Universities (No.CQDXWL-2014-001, No.CDJZR12225501, No.CQDXWL-2013-012).

References

Ding, X. L., C. X. Kan, B. Mo, S. L. Ke, B. Cong, L. H. Xu, and J. J. Zhu. 2012. "Synthesis of Polyhedral Ag Nanostructures by a PVP-Assisted Hydrothermal Method." *Journal of Nanoparticle Research* 14:1000.

Fan, F. R., Z. Q. Tian, and Z. L. Wang. 2012. "Flexible Triboelectric Generator." *Nano Energy* 1:328–34.

Gao, P. X., J. H. Song, J. Liu, and Z. L. Wang. 2007. "Nanowire Piezoelectric Nanogenerators on Plastic Substrates as Flexible Power Sources for Nanodevices." *Advanced Materials* 19: 67–72.

Gu, L., N. Y. Cui, L. Cheng, Q. Xu, S. Bai, M. M. Yuan, W. W. Wu, J. M. Liu, Y. Zhao, F. Ma, et al. 2013. "Flexible Fiber Nanogenerator with 209 V Output Voltage Directly Powers a Light-Emitting Diode." *Nano Letters* 13:91–4.

Guo, H. Y., X. M. He, J. W. Zhong, Q. Zhong, Q. Leng, C. G. Hu, J. Chen, L. Tian, Y. Xia, and J. Zhou. 2014. "A Nanogenerator for Harvesting Airflow Energy and Light Energy." *Journal of Materials Chemistry A* 2:2079–87.

Herb, R. G., D. B. Parkinson, and D. W. Kerst. 1937. "The Development and Performance of an Electrostatic Generator Operating Under High Air Pressure." *Physical Review* 51:75–83.

Jing, Q. S., G. Zhu, P. Bai, Y. N. Xie, J. Chen, P. S. Ray, and Z. L. Wang. 2014. "Case-Encapsulated Triboelectric Nanogenerator for Harvesting Energy From Reciprocating Sliding Motion." *Acs Nano* 8:3836–42.

Jung, J. H., C. Y. Chen, B. K. Yun, N. Lee, Y. S. Zhou, W. Jo, L. J. Chou, and Z. L. Wang. 2012. "Lead-Free KNbO3 Ferroelectric Nanorod Based Flexible Nanogenerator and Capacitors." *Nanotechnology* 23 (37):375401.

Jung, J. H., M. Lee, J. I. Hong, Y. Ding, C. Y. Chen, L. J. Chou, and Z. L. Wang. 2011. "Lead-Free NaNbO3 Nanowires for High Output Piezoelectric Nanogenerator." *Acs Nano* 5 (12):10041–6.

Ke, T. Y., H. A. Chen, H. S. Sheu, J. W. Yeh, H. N. Lin, C. Y. Lee, and H. T. Chiu. 2008. "Sodium Niobate Nanowire and Its Piezoelectricity." *The Journal of Physical Chemistry C* 112: 8827–31.

Ko, Y. H., G. Nagaraju, S. H. Lee, and J. S. Yu. 2014. "PDMS-Based Triboelectric and Transparent Nanogenerators with ZnO Nanorod Arrays." *ACS Applied Materials & Interfaces* 6:6631–7.

Lee, J. H., K. Y. Lee, B. Kumar, N. T. Tien, N. E. Lee, and S. W. Kim. 2013. "Highly Sensitive Stretchable Transparent Piezoelectric Nanogenerators." *Energy & Environmental Science* 6:169–75.

Lin, Z. H., Y. N. Xie, Y. Yang, S. Wang, G. Zhu, and Z. L. Wang. 2013. "Enhanced Triboelectric Nanogenerators and Triboelectric Nanosens or Using Chemically Modified TiO_2 Nanomaterials." *Acs Nano* 7:4554–60.

Mitcheson, P. D., P. Miao, B. H. Stark, E. M. Yeatman, A. S. Holmes, and T. C. Green. 2004. "Mems Electrostatic Micro-Power Generator for Low Frequency Operation." *Sensors and Actuators A: Physical* 115:523–9.

Park, K. I., S. Xu, Y. Liu, G. T. Hwang, S. J. Kang, Z. L. Wang, and K. J. Lee. 2010. "Piezoelectric BaTiO3 Thin Film Nanogenerator on Plastic Substrates." *Nano Letters* 10:4939–43.

Rome, L., L. Flynn, E. M. Goldman, and T. D. Yoo. 2005. "Generating Electricity While Walking with Loads." *Science* 309:1725–8.

Shin, S. H., Y. H. Kim, M. H. Lee, J. Y. Jung, and J. Nah. 2014. "Hemispherically Aggregated $BaTiO_3$ Nanoparticle Composite Thin Film for High-Performance Flexible Piezoelectric Nanogenerator." *Acs Nano* 8 (3):2766–73.

Sun, Y. G., and Y. N. Xia. 2002. "Shape-Controlled Synthesis of Gold and Silver Nanoparticles." *Science* 298:2176–9.

Wang, Z. L. 2014. "Triboelectric Nanogenerators as New Energy Technology and Self-Powered Sensors – Principles, Problems and Perspectives." *Faraday Discuss* 176:447–58.

Wang, Z. L., and J. H. Song. 2006. "Piezoelectric Nanogenerators Based on Zinc Oxide Nanowire Arrays." *Science* 312:242–6.

Williams, C. B., C. Shearwood, M. A. Harradine, P. H. Mellor, T. S. Birch, and R. B. Yates. 2001. "Development of an Electromagnetic Micro-Generator." *IEE Proceedings – Circuits, Devices and Systems* 6:337–42.

Yang, R. S., Y. Qin, C. Li, G. Zhu, and Z. L. Wang. 2009. "Converting Biomechanical Energy into Electricity by a Muscle-Movement-Driven Nanogenerator." *Nano Letters* 9:1201–5.

Yang, Y., H. L. Zhang, J. Chen, Q. S. Jing, Y. S. Zhou, X. N. Wen, and Z. L. Wang. 2013a. "Single-Electrode-Based Sliding Triboelectric Nanogenerator for Self-Powered Displacement Vector Sensor System." *Acs Nano* 7 (8):7342–51.

Yang, Y., H. L. Zhang, Z. H. Lin, Y. S. Zhou, Q. S. Jing, Y. J. Su, J. Yang, J. Chen, C. G. Hu, and Z. L. Wang. 2013b. "Human Skin Based Triboelectric Nanogenerators for Harvesting Biomechanical Energy and as Self-Powered Active Tactile Sensor System." *Acs Nano* 7:9213–22.

Yang, Y., Y. S. Zhou, H. L. Zhang, Y. Liu, S. M. Lee, and Z. L. Wang. 2013c. "A Single-Electrode Based Triboelectric Nanogenerator as Self-Powered Tracking System." *Advanced Materials* 25:6594–601.

Zhang, H. L., Y. Yang, Y. J. Su, J. Chen, K. Adam, S. Lee, C. G. Hu, and Z. L. Wang. 2014a. "Triboelectric Nanogenerator for Harvesting Vibration Energy in Full Space and as Self-Powered Acceleration Sensor." *Advanced Functional Materials* 24: 1401–7.

Zhang, H. L., Y. Yang, X. D. Zhong, Y. J. Su, Y. S. Zhou, C. G. Hu, and Z. L. Wang. 2014b. "Single-Electrode-Based Rotating Triboelectric Nanogenerator for Harvesting Energy From Tires." *Acs Nano* 8:680–9.